

Field-Induced Commensurate-Incommensurate Phase Transition in a Dzyaloshinskii-Moriya Spiral Antiferromagnet

A. Zheludev, S. Maslov, and G. Shirane

Department of Physics, Brookhaven National Laboratory, Upton, New York 11973

Y. Sasago, N. Koide, and K. Uchinokura

Department of Applied Physics, The University of Tokyo, 7-3-1 Hongo, Bunkyo-ku, Tokyo 113, Japan

(Received 8 January 1997)

We report an observation of a commensurate-incommensurate phase transition in a Dzyaloshinskii-Moriya spiral magnet $\text{Ba}_2\text{CuGe}_2\text{O}_7$. The transition is induced by applying a magnetic field in the plane of spin rotation. In this experiment we have direct control over the strength of the commensurate potential, while the preferred incommensurate period of the spin system remains unchanged. Experimental results for the period of the soliton lattice and bulk magnetization as a function of external magnetic field are in quantitative agreement with theory. [S0031-9007(97)03428-5]

PACS numbers: 75.30.Kz

Studies of commensurate-incommensurate (CI) phase transitions have a long history, dating back to the pioneering works of Frenkel and Kontorova [1] and Frank and van der Merwe. [2]. Since then CI transitions were discovered and studied in a number of such seemingly unrelated systems as noble gas monolayers adsorbed on graphite surface [3], charge density wave materials [4], ferroelectrics [5] and rare-earth magnets [6] (for comprehensive reviews, see, for example, Ref. [7]). As a rule, CI transitions result from a competition between two distinct terms in the Hamiltonian that have different “built-in” spatial periodicities and are often referred to as potential and elastic energy, respectively. The potential energy by definition favors a structure commensurate with the crystal lattice. The elastic term is intrinsic to the system where the transition occurs, and has a different “natural” built-in period. In many known realizations of CI, such as adsorbed gas monolayers, it is the period set by the elastic term that can be varied in an experiment to drive the transition. In other systems, such as rare-earth magnets, both the elastic term (exchange coupling between spins) and the potential (magnetic anisotropy) can be changed, but only indirectly, by varying the temperature.

From the very start it was clear that in its purest form a CI transition may be driven by the change of the *strength* of the potential alone, with the two built-in periods remaining constant. An elegant realization of this type of CI was first proposed by Dzyaloshinskii [8], who considered an incommensurate spiral magnetic structure in a magnetic field applied *in the plane of rotation of spins*. In this model incommensurability is intrinsic to the spin system and results from spin-spin interactions. The role of the potential is played solely by an external magnetic field H , which favors a commensurate spin-flop state. In a real magnetic material with this type of CI transition an experimentalist would have a convenient handle on the strength of the potential term, adjusting it by simply changing the magnetic

field. Such systems are not easy to find. In most spiral magnets, e.g., cubic MnSi [9] and FeGe [10], even a small field is sufficient to realign the spin plane *perpendicular* to the field direction. In compounds like RbMnBr_3 [11,12] and CsFeCl_3 [13] the phase behavior is seriously complicated by frustrations inevitably present in a triangular spin lattice. To our knowledge, the most crucial quantities, namely, the incommensurability parameter ζ and magnetization M , have not been measured as a function of the external field in any “clean” realization of Dzyaloshinskii’s model to date. In the present paper we report the first direct experimental observation of a Dzyaloshinskii-type field-induced CI transition in $\text{Ba}_2\text{CuGe}_2\text{O}_7$, also presenting experimental data for $\zeta(H)$ and $M(H)$. On the theoretical side we go beyond a qualitative analysis of the critical properties (close to the phase transition), as was previously done by Dzyaloshinskii [8]. Dealing with this particular system, we construct an exactly solvable model and derive exact results that are in *quantitative* agreement with experiment throughout the *entire* phase diagram.

Structural and magnetic properties of $\text{Ba}_2\text{CuGe}_2\text{O}_7$ are discussed in detail in Ref. [14]. In the layered tetragonal crystal structure the magnetic Cu^{2+} sites form a square lattice with nearest-neighbor (nn) distances of 6 Å along the (1, 1, 0) and (1, -1, 0) directions, respectively. The low-temperature ($T_N = 3.26$ K) magnetic phase is a weak distortion of the Néel spin arrangement, with all spins confined to the (1, -1, 0) plane and the staggered magnetization slowly rotating upon translation along the (1, 1, 0) direction. The propagation vector is $(1 + \zeta, \zeta, 0)$, where $\zeta = 0.027$. Only the nearest-neighbor in-plane antiferromagnetic (AF) exchange constant is significant and is equal to $J_{ab} = 0.48$ meV. The coupling between adjacent Cu planes is ferromagnetic, with $|J_c|/|J_{ab}| \approx 1/37$. We have previously suggested that the incommensurate structure is a result of Dzyaloshinskii-Moriya [15,16] antisymmetric exchange interactions. The corresponding term in

the Hamiltonian can be written as $\mathbf{D}(\mathbf{S}_1 \times \mathbf{S}_2)$, where \times denotes the vector product and \mathbf{D} is a vector associated with the oriented bond between the two interacting spins.

From the symmetry properties of the lattice we deduce that for a bond between two nn Cu sites along the $(1, 1, 0)$ direction, the only allowed components of \mathbf{D} are those along $(1, -1, 0)$ and $(0, 0, 1)$, respectively (Fig. 1). The $(1, -1, 0)$ component does not change sign from one bond to the next, while the $(0, 0, 1)$ component is sign alternating. It is the uniform component that is liable for the incommensurate distortion of the Néel structure, and for the rest of the paper we shall ignore the oscillating component. The interaction energy is minimized when all spins are perpendicular to \mathbf{D} . The total exchange energy of the pair of nearest-neighbor spins is given by $2J_{ab} \cos \phi + D \sin \phi = \sqrt{4J_{ab}^2 + D^2} \cos(\phi - \alpha)$, where ϕ is the angle between spins, and $\alpha = -\arctan D/J_{ab}$. The energy is a minimum at $\phi = \pi + \alpha$. The classical ground state is therefore a spin spiral, with all spins in the $(1, -1, 0)$ plane, and the angle between subsequent spins equal to $\pi + \alpha$. The angle α is related to the propagation vector ζ by $\alpha = 2\pi\zeta \approx 10^\circ$. Precisely this spin configuration was found in the initial zero-field neutron diffraction experiments [14].

The central experimental result of this paper is the observation of a CI transition in $\text{Ba}_2\text{CuGe}_2\text{O}_7$, induced by a magnetic field applied along the $(0, 0, 1)$ direction. Single-crystal magnetization measurements were performed using a conventional dc-SQUID magnetometer in the temperature range 2–300 K. Experimental $\chi(H) \equiv \frac{dM}{dH}$ for $T = 2$ K are shown in Fig. 2. For $\mathbf{H} \parallel \mathbf{a}$ no anomalies are observed. In contrast, when the field is applied along the c axis, a distinct feature is seen around $H = 2$ T and indicates the presence of a magnetic phase transition. Neutron diffraction experiments were carried out on the H9 (cold beam) and H4M (thermal beam) three-axis spectrometers at the High Flux Beam Reactor at Brookhaven National Laboratory on a $\approx 4 \times 4 \times 4$ mm³ single-crystal sample, in the temperature range 1.3–5 K and magnetic fields up to 6.5 T, applied along the c axis of the crystal [17]. In

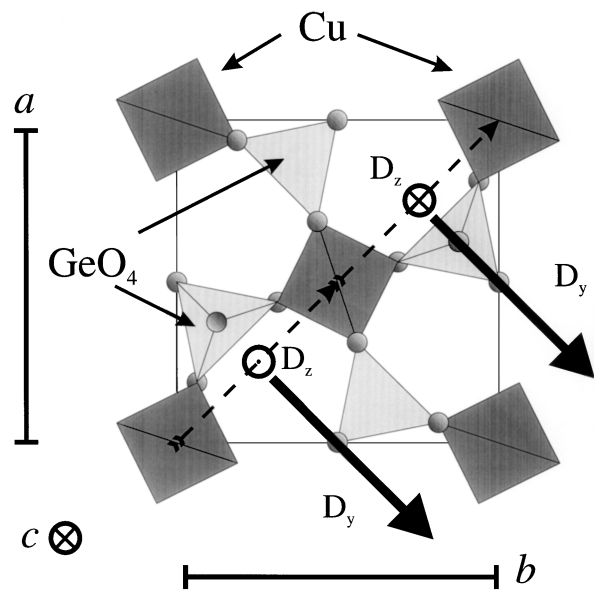


FIG. 1. A schematic view of a Cu-Ge-O layer in $\text{Ba}_2\text{CuGe}_2\text{O}_7$. The arrows indicate the components of Dzyaloshinskii vector \mathbf{D} , allowed by the symmetry.

zero field, at $T = 2.4$ K $< T_N$, elastic scans along the $(1 + \zeta, \zeta, 0)$ direction show magnetic Bragg reflections centered at an incommensurate position $\zeta = \pm 0.0273$ [Ref. [14], Fig. 3(b)]. As the magnetic field increases, the peak moves in closer to the AF zone center at $(1, 0, 0)$ [Fig. 3, inset (a)]. At $H > H_c \approx 2.3$ T the satellites at $(1 \pm \zeta, \pm \zeta, 0)$ are no longer observed, but are replaced by a single peak at the C point $(1, 0, 0)$ [Fig. 3, inset (b)]. The magnetic structure thus becomes commensurate. The experimental field dependence of the propagation vector ζ is shown in the main panel of Fig. 3.

To quantitatively describe the field-dependent behavior, we follow the approach of Dzyaloshinskii [8]. We assume that the vector of local staggered magnetization at point \mathbf{r} remains in the $(1, -1, 0)$ plane and forms angle $\theta(\mathbf{r})$ with respect to the c axis. The free energy per Cu plane in the continuous limit is then given by

$$F = \int \left\{ \frac{\rho_s}{2} \left[\left(\frac{\partial \theta(\mathbf{r})}{\partial x} - \frac{\alpha}{\Lambda} \right)^2 + \left(\frac{\partial \theta(\mathbf{r})}{\partial y} \right)^2 + \gamma \left(\frac{\partial \theta(\mathbf{r})}{\partial z} \right)^2 \right] - \frac{(\chi_\perp - \chi_\parallel)H^2}{2} \sin^2 \theta(\mathbf{r}) \right\} d\mathbf{x} d\mathbf{y}. \quad (1)$$

Here the axes x , y , and z run along the $(1, 1, 0)$, $(1, -1, 0)$, and $(0, 0, 1)$ directions, respectively, and $\mathbf{r} = (x, y, z)$. The first term is the total elastic energy of exchange interactions, and favors a spiral structure of period $\frac{2\pi\Lambda}{\alpha}$. In Eq. (1) Λ is the in-plane nn Cu-Cu distance, and ρ_s is the in-plane spin stiffness, that for classical spins at zero temperature is given by $\rho_s(0) = \sqrt{J_{ab}^2 + D^2} S^2$. γ is the spin stiffness anisotropy defined by $\gamma(\Lambda_c/\Lambda)^2 = |J_c|/|J_{ab}| \approx 1/37$ for $\text{Ba}_2\text{CuGe}_2\text{O}_7$. The second term represents the Zeeman energy. $\chi_\parallel(T)$ and $\chi_\perp(T)$ are defined as magnetic susceptibilities with respect to fields that rotate along with the spiral structure

and are parallel or perpendicular to the local staggered magnetization, respectively. In the paramagnetic phase $\chi_\parallel(T) = \chi_\perp(T)$, while at $T = 0$ the classical result is $\chi_\perp(0) = (g\mu_B)^2/8J_{ab}\Lambda^2$, and $\chi_\parallel(0) = 0$. The equilibrium spin configuration should minimize the free energy (1), and therefore satisfy

$$\frac{\partial^2 \theta}{\partial x^2} = -\frac{(\chi_\perp - \chi_\parallel)H^2}{\rho_s} \sin \theta \cos \theta = -\frac{1}{2\Gamma^2} \sin 2\theta, \quad (2)$$

where $\Gamma = [\rho_s/H^2(\chi_\perp - \chi_\parallel)]^{1/2}$.

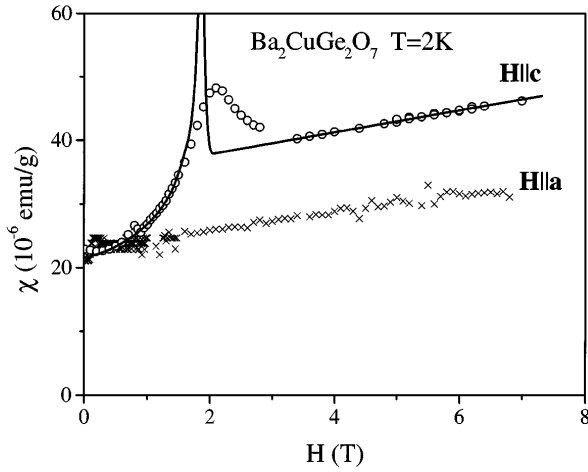


FIG. 2. Field dependence of the magnetic susceptibility measured in $\text{Ba}_2\text{CuGe}_2\text{O}_7$ at $T = 2$ K for the magnetic field applied along the c (circles) and a (crosses) axes of the crystal, respectively. The solid line is a theoretical fit to the data, as described in the text.

Expression (2) has the form of the sine-Gordon equation, which is central to describing CI transitions in many systems, and its “soliton lattice” solutions are well known:

$$\theta(x) = \text{am}(x/\beta\Gamma, \beta), \quad (3)$$

where $\text{am}(x, \beta)$ is the Jacobi elliptic function of modulus β . Analogs of Eqs. (1) and (2) were derived in Ref. [8]. To obtain exact results for $\zeta(H)$ and $M(H)$, however, we make one additional crucial step. For each value of H of all valid solutions, labeled by β , one has to choose the one that indeed corresponds to the global minimum of the free energy. This is done by substituting Eq. (3) into Eq. (1) and minimizing the resulting expression with respect to β . After some algebra we find that F is minimized

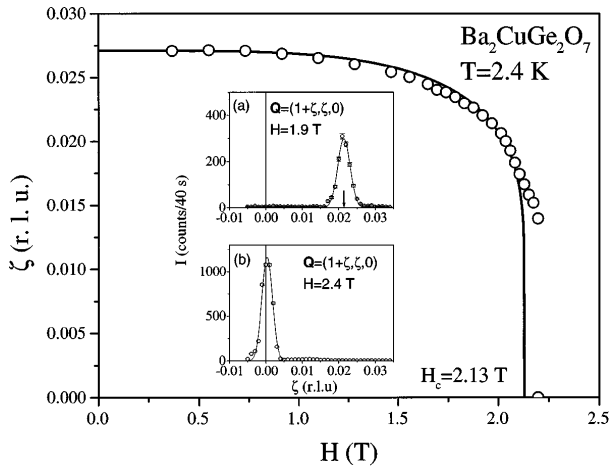


FIG. 3. Field dependence of the magnetic propagation vector in $\text{Ba}_2\text{CuGe}_2\text{O}_7$ measured at $T = 2.4$ K. The solid line is a theoretical fit given by Eqs. (4) and (7). Insets: Elastic scans across the antiferromagnetic zone center for two different values of magnetic field applied along the $(0, 0, 1)$ direction.

when

$$\frac{\beta}{E(\beta)} = \frac{H}{H_c}; \quad (4)$$

$$H_c = \frac{\pi\alpha}{2\Lambda} \sqrt{\frac{\rho_s}{\chi_\perp - \chi_\parallel}}, \quad (5)$$

where $E(\beta)$ is the elliptic integral of the second kind. H_c is the critical field at which the CI transition occurs [8]. Indeed, for $H > H_c$ the spin structure is given by the soliton-free solution $\theta(\mathbf{r}) \equiv \pi/2$, which corresponds to a commensurate spin-flop phase, as visualized in Fig. 4(a). The staggered magnetization in this case is parallel to the x axis and the spins are slightly tilted in the direction of the field. In the limit $H = 0$ one has $\beta \rightarrow 0$ and $\theta(x) = \frac{\alpha}{2\pi} \frac{x}{\Lambda}$, which corresponds to an unperturbed sinusoidal spin spiral [Fig. 4(c)]. Most interesting is the case $0 < H < H_c$, where the spin structure may be described as a soliton lattice: regions of the spin-flop phase are interrupted at regular intervals by magnetic domain walls, or solitons [Fig. 4(b)]. In each soliton the direction of staggered magnetization rotates by an angle π . At $H \rightarrow H_c$, the density of solitons starts to decrease very rapidly, as $1/|\ln(H_c - H)|$ [8]. The transition at H_c is thus almost first order.

The exact expression for $\beta(H)$ [Eq. (4)] enables us to derive parametric equations for the field dependence of M and ζ , and directly compare these predictions to experimental results for $\text{Ba}_2\text{CuGe}_2\text{O}_7$. Using the formula $M = -\partial F/\partial H$ and the equalities for derivatives of elliptic functions [18] one gets

$$M = \chi_\parallel H + (\chi_\perp - \chi_\parallel) H \frac{1}{\beta^2} \left(1 - \frac{E(\beta)}{K(\beta)} \right). \quad (6)$$

The magnetization curve is continuous at the critical field, while $\chi(H) \equiv \frac{dM}{dH}$ diverges as H_c is approached from below, and is constant and equal to χ_\perp at $H > H_c$. In zero field χ is equal to $(\chi_\parallel + \chi_\perp)/2$. We now use Eq. (6) together with the formula (4) to fit the experimental $\chi(H)$ for $\text{Ba}_2\text{CuGe}_2\text{O}_7$ measured at $T = 2$ K. With $\chi_\perp = 3.43 \times 10^{-5}$ emu/g, $\chi_\parallel = 0.89 \times 10^{-5}$ emu/g and $H_c = 1.88$ T a very good fit is obtained (Fig. 2, solid line for

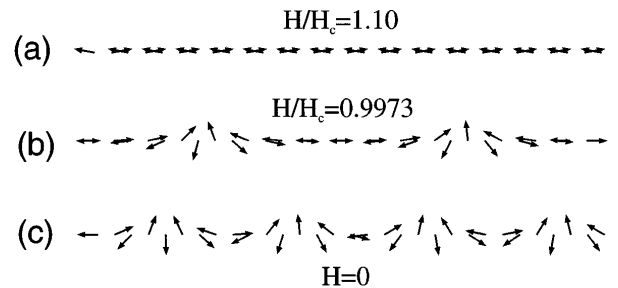


FIG. 4. Spin configurations for the spin-flop phase at $H > H_c$ (a), the soliton lattice at $H = 0.997H_c$ (b), and the circular spin spiral at $H = 0$ (c).

$H \parallel c$). In the refinement we have included a linear contribution to $\chi(H)$, which is apparent in both $\chi_c(H)$ and $\chi_a(H)$. It arises from intrinsic nonlinearities in magnetization curves in the quantum (quasi-) two-dimensional AF Heisenberg model (Ref. [19], especially Fig. 5), that in our case effectively modify the local susceptibilities χ_\perp and χ_\parallel at high fields.

As $H \rightarrow H_c$ the period of the magnetic structure increases. Expressing ζ in terms of β is rather straightforward and yields

$$\frac{\zeta(H)}{\zeta(0)} = \frac{H}{H_c} \frac{\pi^2}{4\beta K(\beta)} = \frac{\pi^2}{4E(\beta)K(\beta)}. \quad (7)$$

Again, Eq. (7), when combined with Eq. (4), gives a parametric curve for $\zeta(H)$, that can be fit to the experimental data for $\text{Ba}_2\text{CuGe}_2\text{O}_7$ using H_c as the only adjustable parameter [$\zeta(0) = 0.027$ is measured independently]. The result with $H_c = 2.13$ T is shown in a solid line in Fig. 3. A remarkable agreement is obtained except very close to H_c . Discrepancies close to the transition point are to be expected, since the transition is almost first order, the soliton lattice is very soft and easily pinned by any impurities. The same effects prevent us from experimentally observing a true divergence in $\chi(H)$ at the critical field (Fig. 2).

Finally, we can estimate the value of the critical field using the previously measured exchange constants and $\zeta(0)$. With $J_{ab} = 0.48$ meV [14] the exchange energy per bond is $\tilde{J} = 2J_{ab}S^2 \approx 0.24$ meV. For χ_\parallel and χ_\perp we can use the values for a classical Heisenberg AF at $T = 0$. ESR measurements [20] provide the gyromagnetic ratios of Cu^{2+} : $g_a = 2.044$ and $g_c = 2.474$. Using Eq. (5) and $\chi_\perp = (g\mu_B)^2/(8J)$ we obtain $H_c = 3.3$ T, which should be compared to the experimental value $H_c \approx 2.1$ T. Considering that in these estimates we have completely ignored quantum and temperature corrections to χ and ρ_s , a 30% consistency is indeed acceptable.

In summary, we have observed a rare type of CI transition that is driven exclusively by the changing strength of the commensurate potential. The latter is directly controlled in an experiment by varying the magnetic field. A transition of this kind was envisioned over three decades ago by Dzyaloshinskii [8], and now we find that $\text{Ba}_2\text{CuGe}_2\text{O}_7$ exhibits it in its original form. Now that the underlying physics is rather well understood, $\text{Ba}_2\text{CuGe}_2\text{O}_7$ can be used as a very neat and simple model system for further studies of spiral magnetism. For example, it would be very interesting to look closer at the magnetic critical behavior.

We thank P. Bak, V. Emery, and I. Zaliznyak for useful discussions. This study was supported in part by NEDO (New Energy and Industrial Technology Development Organization) International Joint Research Grant and the U.S.-Japan Cooperative Program on Neutron Scattering. Work at Brookhaven National Laboratory was supported by the U.S. Department of Energy Division of Material Science, under Contract No. DE-AC02-76CH00016.

-
- [1] Y. Frenkel and T. Kontorova, *Zh. Eksp. Teor. Fiz.* **8**, 1340 (1938).
 - [2] F. Frank and J. van der Merwe, *Proc. R. Soc. London A* **198**, 205 (1949).
 - [3] R. Clarke, in *Ordering in Two Dimensions*, edited by S. Sinha (North-Holland, Amsterdam, 1980), p. 53; H. Zabel, *ibid.*, p. 61.
 - [4] J.A. Wilson, F.J. Disalvo, and S. Mahajan, *Adv. Phys.* **24**, 117 (1975); R.M. Fleming, D.E. Moncton, and D. McWhan, *Phys. Rev. B* **18**, 5560 (1978).
 - [5] A.H. Moudden, E.C. Svensson, and G. Shirane, *Phys. Rev. Lett.* **82**, 557 (1982).
 - [6] W.C. Koehler, in *Magnetic Properties of Rare Earth Metals*, edited by R.J. Elliott (Plenum, New York, 1972), p. 81.
 - [7] P. Bak, *Rep. Prog. Phys.* **45**, 587 (1982); V.L. Pokrovsky, A.L. Talapov, and P. Bak, in *Solitons*, edited by S.E. Trullinger, V.E. Zakharov, and V.L. Pokrovsky (Elsevier Science, Amsterdam, 1986), p. 71.
 - [8] I.E. Dzyaloshinskii, *Sov. Phys. JETP* **20**, 665 (1965).
 - [9] Y. Ishikawa, K. Tajima, D. Bloch, and M. Roth, *Solid State Commun.* **19**, 525 (1976).
 - [10] B. Lebech, J. Bernhard, and T. Flertoft, *J. Phys. Condens. Matter* **1**, 6105 (1989).
 - [11] L. Heller, M.F. Collins, Y.S. Yang, and B. Collier, *Phys. Rev. B* **49**, 1104 (1994).
 - [12] M. Zhitomirsky, O. Petrenko, and L. Prozorova, *Phys. Rev. B* **52**, 3511 (1995).
 - [13] W. Knop, M. Steiner, and P. Day, *J. Magn. Magn. Mater.* **31-34**, 1033 (1983).
 - [14] A. Zheludev *et al.*, *Phys. Rev. B* **54**, 15 163 (1996); see also **55**, 11 879(E) (1997).
 - [15] I. Dzyaloshinskii, *Sov. Phys. JETP* **5**, 1259 (1957).
 - [16] T. Moriya, *Phys. Rev.* **120**, 91 (1960).
 - [17] A complete experimental report will be published elsewhere.
 - [18] S. Gradstein and I. Ryzhik, *Tables of Integrals, Series, and Products* (Academic Press, New York, 1980).
 - [19] K. Fabricius, M. Karbach, U. Löw, and K.-H. Mütter, *Phys. Rev. B* **45**, 5315 (1992).
 - [20] Y. Sasago (unpublished).